WETTING–DEWETTING TRANSITION AND CONFORMAL TO NON-CONFORMAL INTERFACIAL ROUGHNESS TRANSITION IN ULTRA-THIN LIQUID CRYSTAL FILMS ON SOLID SUBSTRATES

K. A. SURESH[*,†], YUSHAN SHI[†], A. BHATTACHARYYA[*] and SATYENDRA KUMAR[*,†]

[*]*Raman Research Institute, Bangalore 560 080, India*
[†]*Department of Physics, Kent State University, Kent, OH 44242, USA*

High-resolution X-ray reflectivity has been employed to study the structure, wetting properties, and interfacial roughness of ultra-thin liquid crystal films. The films were prepared at the air–water interface and transferred on to glass substrates by a modified horizontal deposition technique. A 3-layer film was found to partially-wet the substrate in the nematic and isotropic phases and dewet upon cooling to the crystalline phase. The surface roughnesses at the air-film and the film-glass interfaces exhibited a gradual reversible but hysteretic conformal (strongly correlated) to non-conformal transition between the isotropic and smectic-A phases.

PACS Number(s): 68.15.+e, 68.45.-v, 64.70.Md, 68.18.+p

Interesting and rich phenomenology has been observed at interfaces between solid–liquid and liquid–gas in a variety of systems. Currently, wetting–dewetting and roughness correlations have drawn considerable attention due to their scientific importance and technological applications. For example, in the case of alkanes, continuous and discontinuous wetting–dewetting transitions have been found at the air–alkane[1] and alcohol–alkane[2] interfaces. These transitions are induced by changes in the temperature dependent contact angle. The system has also been reported to exhibit critical wetting[2] involving a continuous and reversible increase in the thickness of an adsorbed film. The most commonly used probes in the past have been ellipsometry,[1,3−5] contact angle measurements,[2,3] optical microscopy,[1,6,7] and X-ray reflectivity.[1,8] Based on the results of these studies, two different mechanisms are believed[6−8] to be responsible for dewetting. In thick films, dewetting is caused by heterogeneous nucleation which results in randomly arranged holes (dewetted regions). On the other hand, destabilizing long range polar interactions cause spinodal dewetting in thin films. This results in holes with short range positional order.

In the case of liquid crystals, due to their anisotropic physical properties, even more interesting and complex phenomena have been observed.[3−5,7−9] The behavior of isotropic fluids and liquid crystalline phases across phase transitions has been

discussed in terms of dewetting, prewetting, partial wetting, complete wetting, and critical wetting. An interesting evolution from the prewetting to non-prewetting state has been observed in a binary mixture of liquid crystals.[4] In this system, a prewetting critical point has also been discovered. The study of wetting properties of ultra thin films of organic materials[10] is very important as they find applications in optical devices, biosensors and lubrication. It is well known that wettability of a solid substrate is dependent on the roughness of the surface.[11] For example, roughness may enhance wetting and thereby shift the wetting transition.[12]

All the liquid crystal films studied so far were either free standing or deposited on substrates by standard techniques such as spin coating. In this letter, we report results on ultra-thin liquid crystal (LC) films of 4′-*n*-octyl-4-cyanobiphenyl (8CB) on glass substrates. These films were first prepared at the air–water interface in a Langmuir trough and transferred on to a glass substrate by a modified *horizontal deposition* technique. This technique yielded well formed monolayer, 3-layer, and multilayer films. Unlike in the usual spincast films, here the absorbate-substrate interaction is through an intermediate absorbate-water interaction arising from trapped water molecules.[13] We studied the interface roughness and the structure in these films by high-resolution X-ray reflectivity. The LC partially wetted the substrate in the nematic and isotropic phases and dewetted on cooling to the crystalline phase. In these ultra-thin films, the (partial) wetting–dewetting transition was found to be reversible. Additionally, the surface *rms* roughnesses in the direction perpendicular to the air-film and film-substrate interfaces became strongly correlated (conformal) in the isotropic and the nematic phases and decorrelated (nonconformal) in the smectic phase. This conformal–nonconformal transition was found to be reversible but hysteretic and first order.

We used 8CB obtained from Aldrich with the phase sequence in the bulk: Crystal 20.5°C Smectic-A 33.3°C Nematic 41.5°C Isotropic. Two-dimensional films of 8CB were prepared at the air–water (AW) interface, by the method described elsewhere.[14] At the AW interface, at room temperature, 8CB exhibits the gas, liquid expanded (monolayer), and multilayer phases.[15] The occurrence of these phases as indicated by surface pressure area isotherm is shown in Fig. 1. Here, the isotherm was obtained at a slow compression rate of 0.05 (Å^2/molecule)/s to get equilibrium structure. Incidentally, the slope of the isotherm between 20 and 48 Å^2 area/molecule (A/M) was very sensitive to the compression rate. Only for fast compressions, which yields non-equilibrium structures, this region was nearly a plateau. The phases were identified by epifluorescence microscopy. It has previously been established[14] that the multilayer domains at the AW interface possess liquid crystalline order.

The usual method to transfer a film from AW interface on to a solid substrate is the vertical dipping Langmuir Blodgett technique. This method does not fully retain the topography of the films as they are affected by gravity. Hence, we employed a horizontal deposition method using a Langmuir trough [see inset in Fig. 1]. Thoroughly cleaned glass plates were placed horizontally below the surface of water.
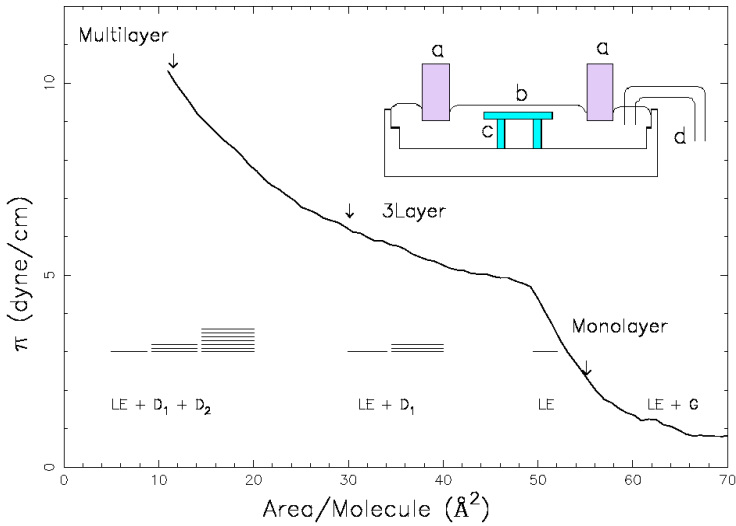
Fig. 1. The surface pressure (π) of 8CB as a function of area per molecule (inverse of surface molecular density) as measured at 25°C. Above 55 Å^2 area/molecule (A/M), the gas (G) and liquid expanded (LE) phases co-exist; the LE phase which is a monolayer exists between 48 and 55 Å^2 A/M; the LE and 3 layer (D_1) phases co-exist between 20 and 48 Å^2 A/M; the multilayer (D_2), D_1, and LE phases co-exist below 20 Å^2 A/M. The structures of the phases in three different regions are also symbolically shown. The inset schematically shows the the horizontal deposition; *a*: barriers, *b*: monolayer, *c*: substrate, and *d*: siphon.

The Langmuir films of 8CB were prepared on the surface of water. Then, the sub-phase (water) was siphoned out drop by drop, thereby slowly lowering the height of the interface. The advantage of this method is that during this process, the domains could be observed continuously by epifluorescence microscope. Any deformation in the structure and topography of the domains could be directly seen while they are being transferred to a substrate. Special precautions were taken to avoid any contamination and even the slightest vibrations of the AW interface which other-wise resulted in deformation of the film. A successful and neat transfer to the glass substrate was confirmed by epifluorescence and polarizing microscopy.

We employed high-resolution X-ray reflectivity to investigate the structure and surface morphology of these ultra-thin films. Measurements were carried out using the Cu-Kα doublet of an 18 kW rotating anode X-ray source and a pair of Ge(111) single crystals as monochromator and analyzer. The details of the reflectivity tech-nique, the experimental setup, and data analysis can be found elsewhere.[16] It is important to note that, only the information about the period and the presence or absence of Kiessig fringes in X-ray reflectivity scans is used in discussions and inferences drawn in this paper. This information can be gleaned from the reflectiv-ity profiles even without exhaustive modeling and fits to the reflectivity. We have used the simplest fits to calculate the period and the approximate roughness. Im-proved fits, which are certainly possible to obtain with more rigorous modeling of the electron density, would not alter these semi-quantitative conclusions.

The X-ray specular reflection measurements were carried out on different types of films transferred to glass plates. In particular, we made measurements on the following:

(i)   the *monolayer*; the LE phase at 52 Å^2 A/M,

(ii) the *3-layer film*; a 3-layer (D_1) covering $\sim 60\%$ of area coexisting with the LE phase at 30 Å^2 A/M,

(iii) the *dense 3-layer film*; films deposited one on top of the other with predominantly D_1 phase ($\sim 90\%$) with traces of LE phase and multilayer domains (D_2), and

(iv) the *multilayer film*; D_2 with D_1 in the background and traces of LE phases at 10 Å^2 A/M.

We measured the specular and diffuse scattering from these films as a function of temperature measured to a precision of $\pm 0.1°$C. As we discuss later, we conclude that the 3-layer films on glass substrates, in all of the above cases undergo transitions in the proximity of 21, 34, and 43°C. From the phase sequence of bulk 8CB, we believe these transitions to be the crystal–smectic-A, the smectic-A–nematic, and the nematic–isotropic phases.

Figure 2 shows the X-ray reflectivity from the above listed four types of films and the bare substrate at room temperature. The thickness of the monolayer film (type (i)) was determined to be 14 Å from the well developed Kiessig fringes. The thickness of the 3-layer film was 44 Å. The fits to the reflectivity profile indicated a coverage of 60% by the 3-layer phase. For the dense 3-layer film, the coverage was $\sim 90\%$ as evident from the more pronounced Kiessig fringes. In the reflectivity profiles of these two films, the Bragg peak corresponding to smectic-A order was not observed due to the film's small thickness. In the multilayer film, the presence of pronounced smectic Bragg peak corresponding to the (bi)layer spacing of 32.3 Å was observed.

The specular reflectivity for the 3-layer film was measured at different temperatures to determine if the film was stable with changes in temperature and liquid crystalline phase transitions. The profile of the specular reflectivity was found to remain essentially the same in the smectic-A, the nematic, and the isotropic phases. These results confirmed the stability and integrity of the 3-layer film. The specular reflectivities of the multilayer film as it was cooled from the nematic phase to the smectic-A and crystalline phases are shown in Fig. 3. These films were found to consist partly of thick multilayer (D_2) domains and a 3-layer film (D_1) covering the remaining area. The coverage of the multilayer domains in this particular film was estimated to be 25%. The Kiessig fringes in the smectic and the nematic phases corresponded to the thickness of 44 Å and were essentially the same as observed for the 3-layer film. The Bragg peak arising from multidomains can be seen in the smectic and crystalline phases. It was found that on cooling to the crystalline phase, the fringes corresponding to 3-layer film disappeared due to dewetting. On heating, the fringes began to reappear confirming the recovery of the 3-layer film at
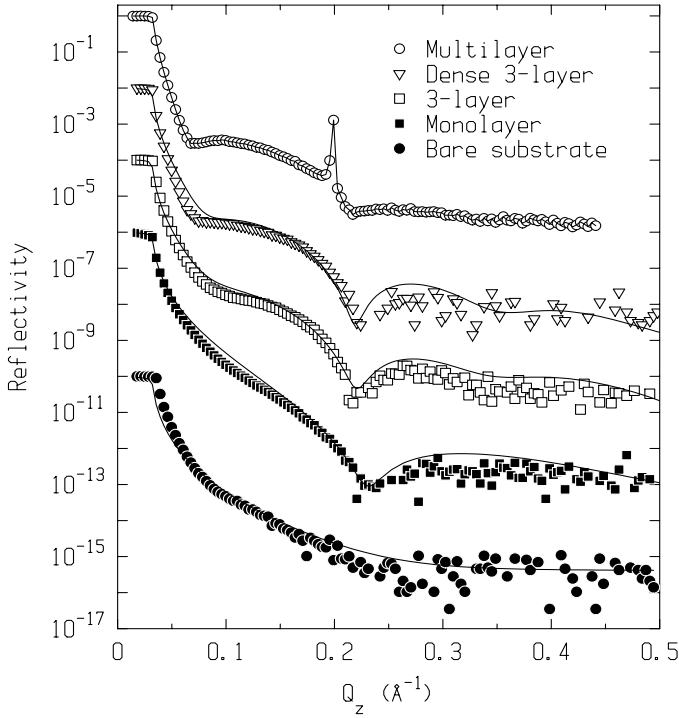
Fig. 2.   X-ray reflectivity of bare substrate (with typical *rms* roughness = 6 Å), monolayer, 3-layer, dense 3-layer, and multilayer films, after subtraction of diffuse scattering and correction for changing footprint of the X-ray beam on the sample. The curves have been shifted down by an integer number of decades for clarity. The measurements were made at room temperature. Solid lines represents the fits used to calculate the film thickness from the period of Kiessig fringes.

temperatures corresponding to the smectic-A phase. Further, in the nematic phase the recovery of this film continued and the fringes fully reappeared in the isotropic phase. The smectic Bragg peak intensity and the amplitude of Kiessig fringes during heating cycle were found to be lower than those during the cooling cycle because of excessive misorientation caused by the crystallization process. The intensities recover if the sample is left in the isotropic phase for a long time. These results show a reversible partial wetting–dewetting transition as a function of temperature which was also confirmed by epifluorescence microscopy. We were able to see very faint wavefronts moving towards LC islands suggesting that the film was retracting into these islands as the crystalline phase was approached. The film was found to reappear upon warming.

   We measured diffuse (non-specular) scattering by longitudinal scans at $\omega = 0.02°$ to determine the changes in conformality of the air-film and film-substrate interfaces. Here ω is the angle by which the sample has been rotated away from the specular condition. The results for the dense 3-layer film and the multilayer film are shown in Fig. 4. In the isotropic phase at 43°C (Fig. 4(a)), the diffuse
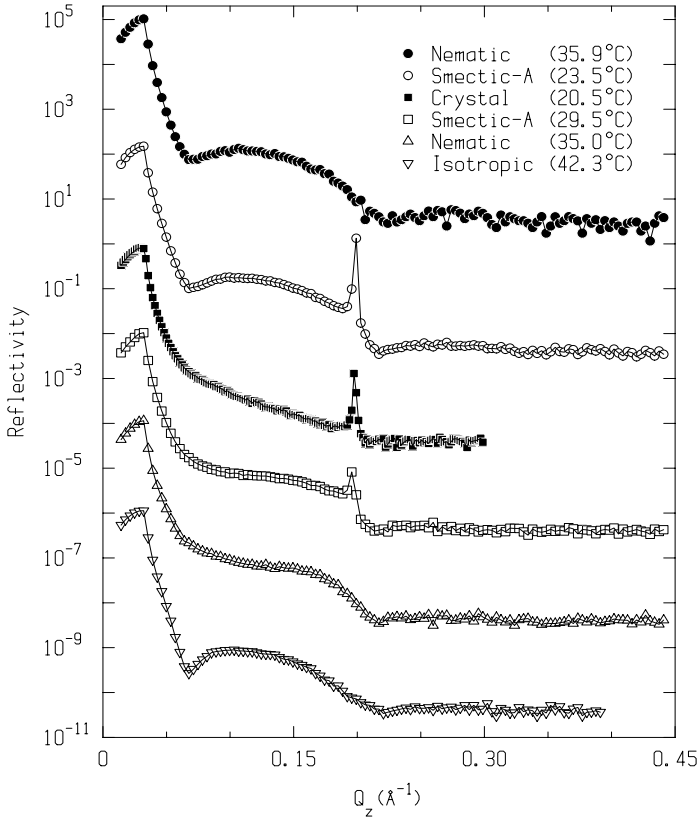
Fig. 3.   Specular reflectivity of multilayer film (type (iv)) without footprint correction at different temperatures, plotted after shifting by integer number of decades for clarity. The Kiessig fringes visible in the nematic and smectic-A phases correspond to 3-layer film which wets the substrate. The Bragg peak in the smectic and crystalline phases arises due to the multilayer domains.

scattering had the signature of the Kiessig fringe observed in the specular reflectivity. This indicated that the roughnesses at the air-film interface conforms[17] to the film-substrate interface roughness. Measurements in the nematic phase led us to the same conclusion. The amplitude of the Kiessig fringe in the off-specular scans began diminishing upon entering the smectic-A phase. As shown in Fig. 4(b), this feature was almost completely lost at 30°C indicating that the roughness of the two interfaces became nonconformal. Identical results were obtained in the case of multi-layer films as shown in Figs. 4(c) and (d). Clearly, the Bragg peak visible in the scan shown in Fig. 4(d) arise from smectic layers in the multi-layer domains. This peak was very sharp and had a FWHM $\sim 0.005°$ in ω-scans which is much smaller than the value of $\omega = 0.02°$ used for off-specular scans. Consequently, the smectic-A peak is not seen in the off-specular scan in Fig. 4(d). The loss of conformality in the smectic-A phase is puzzling since the film still wets the substrate and elasticity of smectic-A should demand conformality.[18]
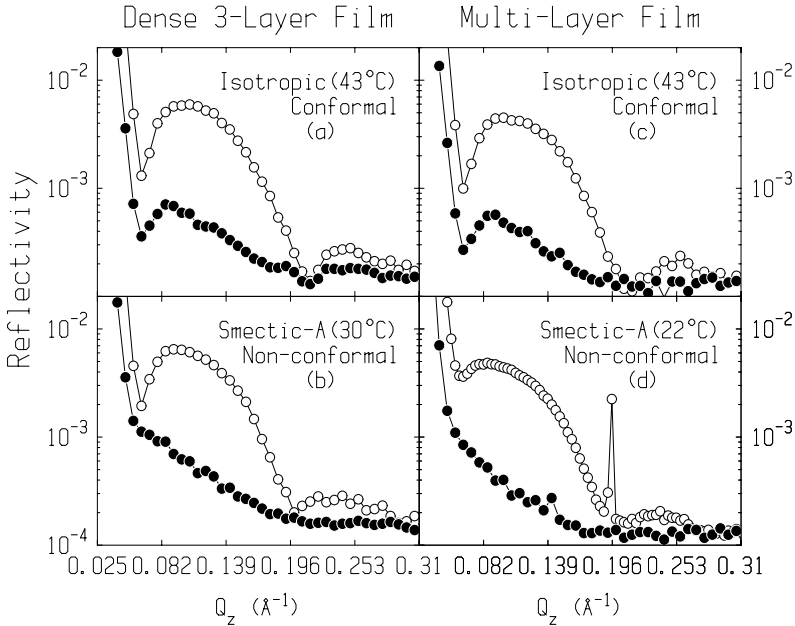
Fig. 4. Specular (◦) and off-specular (•) reflectivity (or diffuse scattering) scans at $\omega = 0.02°$ for a dense 3-layer (type (iii)) and multi-layer (type (iv)) films. In the isotropic phase at $43°$C (in (a) and (c)), the off-specular scattering has similar profile as the specular reflection as they both show Kiessig fringes indicating that the air-LC and LC-substrate interfaces have the same *rms* roughness, i.e. they are conformal. However, in the smectic-A phase (in (b) and (d)), the fringes have disappeared in the off-specular scans indicating non-conformal roughnesses at the two interfaces. In Fig. 4(d), the nearly resolution limited Bragg peak disappears in the off-specular scans conducted at $0.02°$.

A simple way to quantitatively specify the degree of conformality at different temperatures is to determine, from line-shape analysis, the amplitude of the Kiessig fringes in the diffuse scattering relative to their (maximum) amplitude in the isotropic phase. This amplitude ratio, which is a measure of the degree of conformality, is shown in Fig. 5 as a function of temperature for the multilayer film. It should be pointed out that each specular and off-specular scan took several hours to complete and a full set of measurements on one sample took several days. The slow pace of data acquisition ensured that the sample had reached equilibrium at each temperature.

It can be seen from the figure, that there are three temperatures (~ 21, 34, and $43°$C) where clear changes in the temperature dependence of the degree of conformality occur. These correspond to the transition in the bulk 8CB albeit at somewhat higher temperatures. Clearly, these changes are occurring at the three associated phase transitions in the 3-layer film. Interestingly, the interface conformality was gradually lost in the smectic-A phase upon cooling. On subsequent heating, it began to recover in the nematic phase and was fully recovered only in the isotropic phase, thus showing a hysteretic behavior.
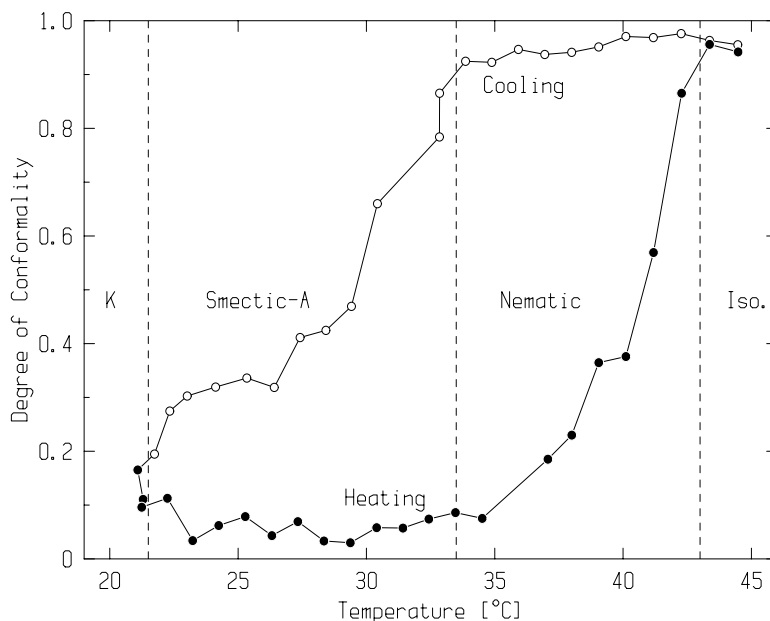
Fig. 5.   Degree of conformality as a function of temperature for the multilayer film (D_2 domains with D_1 in the background). On cooling, the roughnesses of the D_1 film remains conformal in the isotropic and nematic phases. The conformality is lost in the smectic and crystalline phases. On heating, conformality is fully recovered in the isotropic phase.

To summarize, we have reported successful transfer of ultra-thin films of 8CB prepared at the AW interface to glass substrates by a modified horizontal deposition technique. High-resolution X-ray reflectivity study has revealed two interesting first order transitions that occur as a function of temperature. We observed partial wetting–dewetting across the smectic-A to crystalline phase transition. These films undergo a first order conformal to nonconformal interface roughness transition in the vicinity of the nematic to smectic-A transition.

Acknowledgments

References

1. C. Merkl, T. Pfohl and H. Riegler, *Phys. Rev. Lett.* **79**, 4625 (1997).
2. D. Ross, D. Bonn and J. Meunier, *Nature* **400**, 737 (1999).
3. F. Vandenbrouck, S. Bardon, M. P. Valignat and A. M. Cazabat, *Phys. Rev. Lett.* **81**, 610 (1998).
4. R. Lucht, Ch. Bahr, G. Heppke and J. W. Goodby, *J. Chem. Phys.* **108**, 3716 (1998); R. Lucht and Ch. Bahr, *Phys. Rev. Lett.* **78**, 3487 (1997); *ibid.* **80**, 3783 (1998).

5. M. P. Valignat, S. Villette, J. Li, R. Barberi, R. Bartolino, E. Dubois-Violette and A. M. Cazabat, *Phys. Rev. Lett.* **77**, 1994 (1996).
6. U. Thiele, M. Mertig and W. Pompe, *Phys. Rev. Lett.* **80**, 2869 (1998).
7. S. Hermninghaus, K. Jacobs, K. Mecke, J. Bischof, A. Fery, M. Ibn-Elhaj and S. Schlagowski, *Science* **282**, 916 (1998).
8. A. L. Demirel and B. Jerome, *Europhys. Lett.* **45**, 58 (1999); B. Jerome, *Mol. Cryst. Liq. Cryst.* **212**, 21 (1992).
9. G. de Crevoisier, P. Fabre, J.-M. Corpart and L. Leibler, *Science* **285**, 1246 (1999).
10. A. Ulman, *An Introduction to Ultra-thin Organic Films* (Academic Press, San Diego, CA, 1991).
11. D. Beaglehole, E. Z. Radlinska, B. W. Ninham and H. K. Christenson, *Phys. Rev. Lett.* **66**, 2084 (1991).
12. R. Netz and D. Andelman, *Phys. Rev.* **E55**, 687 (1997).
13. M. N. G. de Mul, J. A. Mann Jr., *Langmuir* **10**, 2311 (1994).
14. K. A. Suresh and A. Bhattacharyya, *Langmuir* **13**, 1377 (1997).
15. A. Bhattacharya and K. A. Suresh, *Europhys. Lett.* **41**, 641 (1998).
16. Y. Shi, B. Cull and S. Kumar, *Phys. Rev. Lett.* **71**, 2773 (1993); B. Cull, Y. Shi and S. Kumar, *Phys. Rev.* **E51**, 526 (1995).
17. S. K. Sinha, *Liquid Crystals: Experimental Study of Physical Properties and Phase Transitions*, ed. S. Kumar (Cambridge Univ. Press, Cambridge, 2000), Chap. 9.
18. P. G. de Gennes and J. Prost, *The Physics of Liquid Crystals*, 2nd edn. (Oxford Univ. Press, Oxford, 1993).